

Preclinical validation of the hypoxia tracer 2-(2-nitroimidazol-1-yl)-N-(3,3,3-[¹⁸F]trifluoropropyl)acetamide, [¹⁸F]EF3

P. Mahy¹, M. De Bast¹, P. H. Leveque^{2, 3}, J. Gillart², D. Labar², J. Marchand⁴, V. Gregoire¹

¹ Department of Radiation Oncology and Radiobiology Unit, Université catholique de Louvain, St-Luc University Hospital, Brussels, Belgium

² Laboratory of Positron Emission Tomography, Université catholique de Louvain, Louvain-la-Neuve, Belgium

³ Laboratory of Pharmaceutical Chemistry and Radiopharmacy, Université catholique de Louvain, Brussels, Belgium

⁴ Department of Organic Chemistry, Université catholique de Louvain, Louvain-la-Neuve, Belgium

Received: 10 February 2004 / Accepted: 13 April 2004 / Published online: 10 June 2004

© Springer-Verlag 2004

Abstract. The 2-nitroimidazole derivative 2-(2-nitroimidazol-1-yl)-N-(3,3,3-trifluoropropyl)acetamide (EF3) is a marker which forms adducts into hypoxic cells. Radiosynthesis of [¹⁸F]EF3 was recently performed by our group. Our aim was to study the pharmacokinetics, biodistribution, metabolism and specificity for hypoxia of [¹⁸F]EF3. MCa-4, SCC VII, NFSA, FSA, FSA II or Sa-NH tumour-bearing C3H mice were injected intravenously with [¹⁸F]EF3 and allowed to breathe air, 10% O₂ or carbogen until sacrifice 5–770 min after injection. Radioactivity was measured *ex vivo* in various organs, including urine and faeces. Selected organs were additionally processed to measure tracer metabolites with high-performance liquid chromatography. The half-life in blood was 73.9 min. [¹⁸F]EF3 was eliminated mainly via the kidneys, with 75% of the injected activity found in the urine by 12 h 50 min. The biodistribution was fast and homogeneous except in the brain and the bone, where it was significantly lower, and in the liver and the kidney, where it was significantly higher. In most organs, the exceptions being the gastrointestinal and urinary tract, tissue-to-blood ratios were below or close to unity. In tumours, a relative accumulation of the tracer was observed with time, which, at 220 min after injection, depended on tumour strain and oxygenation conditions, i.e. 10% O₂ significantly increased the tumour-to-muscle ratio whereas carbogen decreased it. [¹⁸F]EF3 was rapidly metabolised in the kidney and the liver. [¹⁸F]EF3 is a promising tracer for detection of tumour hypoxia. A phase I study in head and neck cancer patients is in progress at our institution.

Keywords: Drug evaluation, preclinical – Hypoxia – Nitroimidazoles – PET – Pharmacokinetics

Eur J Nucl Med Mol Imaging (2004) 31:1263–1272
DOI 10.1007/s00259-004-1573-2

Introduction

Hypoxia is known to be an important prognostic factor in human oncology. Several studies conducted in different tumour types have demonstrated a correlation between the probability of loco-regional recurrence and/or the probability of overall survival, and tumour hypoxia as measured with Eppendorf probes [1]. The use of polarographic electrodes is, however, invasive and limited to superficial tumours or nodes, which is likely to restrict its clinical implementation on a routine basis. Furthermore, tumour necrosis tends to artificially lower the readings, and even if multiple tracks are used, the measurements may not sample the whole tumour.

The use of 2-nitroimidazole derivatives (e.g. pimonidazole, NITP, EF3, EF5) represents an attractive alternative to polarographic measurements [2–5]. These compounds undergo intracellular chemical reduction, and under hypoxia their reduced moieties covalently bind to macromolecules, mainly to thiol-containing proteins [6]. The adducts hence trapped into hypoxic cells can be detected either by immunohistochemistry [2, 7] or immunofluorescence on tissue sections [4, 5], or by flow cytometry on cell suspensions [5], specific antibodies being used for both techniques. In head and neck squamous cell carcinoma, pimonidazole binding, as detected by immunohistochemistry, has been demonstrated to predict treatment outcome [7]. A recent report also indicated that EF5 binding, as detected by immunofluorescence, was predictive for recurrence in adult brain tu-

V. Gregoire (✉)

Department of Radiation Oncology and Radiobiology Unit,
Université catholique de Louvain, St-Luc University Hospital,
10 Ave Hippocrate, 1200 Brussels, Belgium
e-mail: gregoire@rbnt.ucl.ac.be
Tel.: +32-2-7649443, Fax: +32-2-7649425

mours treated by surgery and postoperative radiotherapy [8]. However, as with the polarographic methods, such measurements are invasive and typically only probe a small fraction of the tumour volume.

Another possible method to detect nitroimidazole adducts is the use of radiolabelled tracers. This approach has some intrinsic advantages, including the non-invasiveness of the method, its repeatability and the possibility of evaluating the whole tumour and of assessing its heterogeneity. Since the first reports on the use of a labelled metronidazole to image abscesses and tumours [9, 10], several ^{123}I - or ^{99}Tc -labelled compounds have been synthesised and validated in preclinical and early clinical studies [11]. Hypoxia tracers labelled with a positron emitter, which have the intrinsic advantage of a better spatial resolution and a more accurate quantitation of the signal, have also been synthesised. ^{18}F fluoromisonidazole (F-MISO) was the first labelled nitroimidazole compound detected by positron emission tomography (PET) [12]. It has been evaluated for detection of hypoxia in experimental [13, 14] and human tumours [15–19], as well as in normal tissues like myocardium [20] and the central nervous system [21] and even in anaerobic odontogenic infections in the jaw [22]. More recently, other ^{18}F -labelled compounds have been synthesised and validated [23, 24]. Among them, ^{18}F fluoroerythronitroimidazole (FETNIM) has been used to detect hypoxia in human head and neck squamous cell carcinoma; tumour-to-plasma ratios slightly above unity have been reported at late time points after tracer injection [25, 26].

All the PET tracers mentioned above are hydrophilic compounds, which might limit their diffusion into tissues, and in particular into tumours which typically have an abnormal vascularisation [27]. In this regard, the class of fluorinated etanidazole compounds (e.g. EF3 and EF5) developed by Koch are of potential interest [4, 5]. These compounds are more lipophilic with an octanol-to-water partition coefficient of 5.7 for EF5 [28]. Preliminary rat experiments with ^{18}F EF5 demonstrated that the tracer was evenly distributed in normal tissues, mainly eliminated through the urinary tract and accumulated in the hypoxic Morris 7777 rat tumour [28]. On the other hand, ^{18}F EF1, which is the most hydrophilic compound of that class (with an octanol-to-water partition coefficient of 0.35), had a more heterogeneous biodistribution. However, it also accumulated in the Morris 7777 rat tumour [29].

Recently, our group labelled the tri-fluorinated etanidazole derivative, 2-(2-nitroimidazol-1-yl)-*N*-(3,3,3- ^{18}F trifluoropropyl)acetamide (^{18}F EF3) [30]. Due to the half-life of ^{18}F , i.e. 110 min, the ability to detect hypoxic tumours with PET will probably result from a balance between a fast and even biodistribution of the tracer (enhanced with lipophilic compounds) and a rapid elimination (facilitated by hydrophilic compounds). In this respect, ^{18}F EF3 might represent a good compromise. In

this study, we investigated the pharmacokinetics, biodistribution, metabolism and hypoxia-dependent binding of ^{18}F EF3 in *in vivo* murine tumour models.

Materials and methods

Drug synthesis

The synthesis of ^{18}F EF3 was adapted from the previously described method [30]. Briefly, the first step was the radiolabeling of poly(hydrogen fluoride) pyridinium, the perfluorinating agent, from isotopic exchange with potassium ^{18}F fluoride under anhydrous conditions. This agent was then used to perfluorinate an aminodithioester precursor whose amine function was protected by a phthalimido group. This radiolabelled precursor was then deprotected and coupled to 2-nitroimidazole acetic acid to generate ^{18}F EF3. ^{18}F EF3 was isolated by reverse phase semi-preparative high-performance liquid chromatography (HPLC) using an aqueous NaH_2PO_4 (1.38 g/l)/acetonitrile mixture (7/3) as eluent. Acetonitrile was removed by evaporation (<400 ppm).

On average, the daily production of ^{18}F EF3 reached an activity of 504 ± 254 MBq (range 155–1,110 MBq). Gamma counting of HPLC fractions of ^{18}F EF3 solution demonstrated a radiochemical purity of $97.7\% \pm 1.5\%$ (mean \pm SD). Specific activity was typically in the order of 150 MBq/mmol.

Animal and tumour models

Eight to twelve-week-old male C3H/HeOulco mice purchased from IFFA CREDO, Belgium were used. Animals were maintained in a facility approved by the Belgian Ministry of Agriculture in accordance with current regulations and standards. Animals were given food and water *ad libitum* for the duration of the experiments. Experimental design was approved by the ethics committee on animal experimentation of the medical school of the Université catholique de Louvain. The “Principles of laboratory animal care” (NIH publication no. 86-23, revised 1985) were strictly followed.

FSA, FSA II, Sa-NH and NFSA fibrosarcomas and MCA-4 and SCC VII carcinomas syngeneic to C3H/Kam mice were used. These tumours were kindly provided by Dr. L. Milas from the University of Texas, M.D. Anderson Cancer Center, Houston, USA. Maintenance and expansion of the tumours *in vivo* have been previously described [31, 32]. Briefly, after thawing in McCoy medium, tumour cells from the third to fifth isograft generations were injected into the mouse flank to generate subcutaneous (SC) tumours. Intramuscular (IM) tumours were generated by injection in the gastrocnemius muscle of 5×10^5 – 10^6 cells in 10–20 μl of McCoy medium. Tumour growth was determined by daily measurements of three orthogonal diameters with a caliper.

Pharmacokinetics and biodistribution experiments were performed on SC FSA II (average tumour weight \pm 1 SD of 1.62 ± 1.09 g) or Sa-NH (average tumour weight \pm 1 SD of 0.35 ± 0.25 g) tumour-bearing mice. Experiments on the tracer metabolism were performed on SC NFSA (average tumour weight \pm 1 SD of 0.23 ± 0.14 g) tumour-bearing mice. Experiments on the ranking of hypoxia among various tumour types were performed on 8–9 mm mean diameter IM FSA (average tumour weight \pm 1 SD of 0.67 ± 0.14 g), FSA II (average tumour weight \pm 1 SD of 0.69 ± 0.20 g), Sa-NH (average tumour weight \pm 1 SD of

0.79±0.34 g), NFSa (average tumour weight ± 1 SD of 0.87±0.20 g), MCa-4 (average tumour weight ± 1 SD of 0.52±0.22 g) and SCC VII (average tumour weight ± 1 SD of 0.80±0.26 g) tumour-bearing mice. Experiments with carbogen and 10% O₂ were performed on IM FSA II and SCC VII tumour-bearing mice.

Experimental design

Mice were injected intravenously in the tail vein with [¹⁸F]EF3. Depending on the design of the experiment, the injected radioactivity varied from 1.8 to 40 MBq (equivalent to a whole-body concentration of 0.5–10 μM of EF3). Such variation in tracer concentration has no influence on its biodistribution. It was demonstrated that the use of an excess amount of unlabelled EF5 (whole body concentration of 100 μM) co-injected with [¹⁸F]EF3 did not modify the pharmacokinetics of the tracer (data not shown). After injection, mice were housed in individual cages adapted for collection of excrement (urine and faeces). When modification of tumour hypoxia was required, carbogen (95% O₂ and 5% CO₂) or 10% O₂ was flowed through the cage at a constant rate of 3 l/min.

[¹⁸F]EF3 assay

For biodistribution and pharmacokinetics experiments, animals were sacrificed by cervico-cranial dislocation at 5, 30, 55, 110, 220, 330, 440, 550, 660 or 770 min after tracer injection. Blood (collected through cardiac puncture just before sacrifice of the animal), emptied bladder, brain, femoral bone, heart (flushed), kidney, large bowel, liver, lung, muscle, oesophagus, tumour, small bowel, spleen and stomach were harvested, weighed and counted for radioactivity. For experiments on the ranking of hypoxia among various tumour types, blood, liver, gastrocnemius muscle (contralateral to tumour-bearing limb) and tumour were harvested. Contamination between organs when handling samples was carefully avoided. A fraction of blood sample was also centrifuged to measure the radioactivity in the serum. For the stomach, small and large bowel, radioactivity was also measured after flushing the organs with saline to get rid of the content (food or faeces). To determine the route of [¹⁸F]EF3 excretion, urine and faeces of individual mouse were collected at 55, 110, 220, 330, 440, 550, 660 and 770 min after tracer injection, and counted for radioactivity.

Samples with very high activity (i.e. urine and faeces) were counted in an ionisation chamber calibrated for ¹⁸F spectrum, whereas all the other samples were counted with a gamma counter (Cobra II Autogamma, Packard Instrument Company). All data were corrected for ¹⁸F decay and expressed as the percentage of injected radioactivity per gram of tissue (%ID/g), tumour-to-blood ratio (TBR) or tumour-to-muscle ratio (TMR).

Analysis of tracer metabolites

The respective proportion of metabolites and native EF3 was measured in the acetonitrile-soluble fraction of various samples. Organs were homogenised in 5 ml of phosphate buffer. Serum and urine were mixed in 1 volume of acetonitrile–10% TCA and in 1 volume of 10% TCA, respectively. After centrifugation, acetonitrile-soluble fractions were collected and concentrated ten times by evaporation. Samples were analysed by HPLC (Dionex DX 300 system) on an Alltima C18 column (Alltech). The eluent was

a mixture of ammonium acetate/acetonitrile with a flow rate of 1 ml/min. Consecutive 3-min HPLC fractions were collected up to 15 min and gamma counted (Cobra II Autogamma, Packard Instrument Company). This method was considered more sensitive than UV detection or online gamma detection.

Data analysis

Pharmacokinetics curves of [¹⁸F]EF3 in blood and serum were fitted using a mono-exponential elimination model (SPSS 10 for Macintosh, SPSS). The statistical difference between several groups of data (e.g. %ID/g in several organs) was assessed using ANOVA and *F* tests. The statistical difference between two groups of paired data (e.g. %ID/g in the large bowel before and after flushing) was assessed using a Student's paired *t* test. The statistical difference between two groups of unpaired data (e.g. %ID/g in organ under 21% or 10% O₂) was assessed using a two-tailed *t* test on the mean. Throughout the experiments, statistical significance was set for a *p* value equal to or lower than 0.05.

Results

Blood pharmacokinetics and elimination

[¹⁸F]EF3 concentrations in blood and serum exhibited a monophasic decline with time after tracer injection, and a mono-exponential elimination model was therefore used to fit the data. In blood, the elimination half-life reached 73.9 min (95% CI: 67.1–82.3 min) (Fig. 1). The pharmacokinetics of [¹⁸F]EF3 was apparently slightly slower in serum, with an elimination half-life of 92.7 min (95% CI: 89.7–95.9 min). This figure was, however, calculated from data obtained from 30 to 330 min after tracer injection. When data in blood were also modelled from 30 to 330 min, an elimination half-life of 84.5 min (95% CI: 78.4–91.6 min) was obtained. This figure was not significantly different from the value in serum.

[¹⁸F]EF3 was predominantly eliminated in the urine via the kidneys and to a lesser extent in the faeces via the gastrointestinal tract (Fig. 2). By 12 h 50 min after injection, 75% and 16% of the injected radioactivity had been collected in the urine and the faeces, respectively.

Biodistribution in normal tissues

The biodistribution of [¹⁸F]EF3 was fast and even throughout the body, except in the brain and the femur, where it remained significantly lower (*p*<0.01 at 5 min in both organs), and in the liver and the kidneys, where it remained significantly higher (*p*<0.01 at 5 min in both organs) (Table 1). In all organs except the large and small bowel, the brain and the femur, the maximum concentration of the tracer peaked as early as 5 min after injection and then progressively decreased. For the latter three organs, the maximum concentration peaked at 55 min after injection. In the small and large bowel, sur-

Fig. 1. Pharmacokinetics of [^{18}F]EF3 in blood. Data points represent the mean \pm 1 SD from four to eight different mice

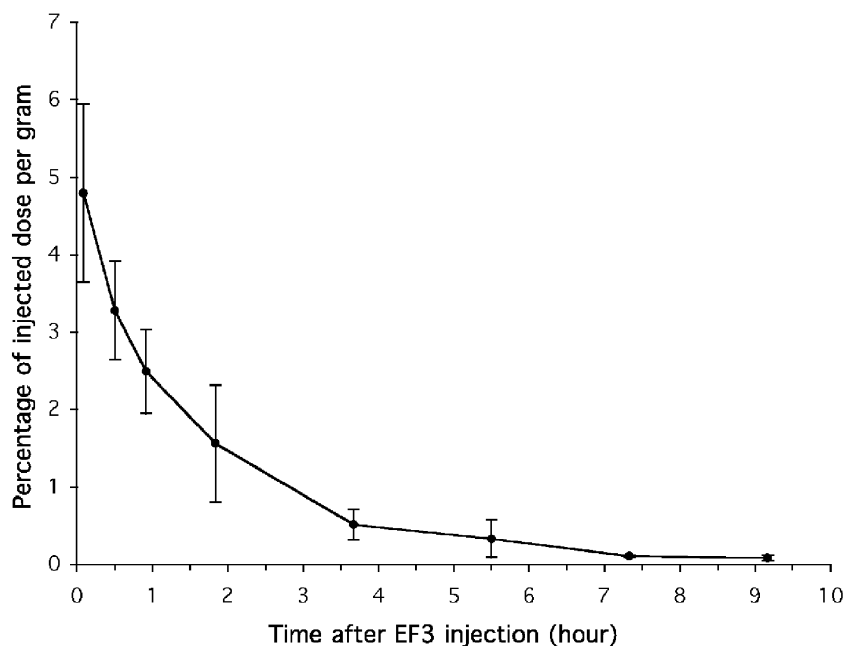
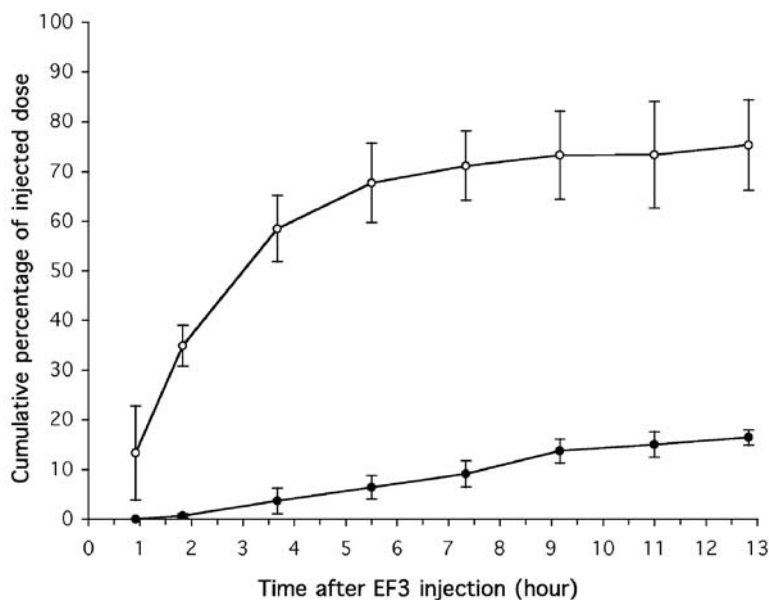


Fig. 2. Excretion of [^{18}F]EF3 in the urine (*open circles*) and faeces (*filled circles*). Data points represent the mean \pm 1 SD from four different mice



prisingly, progressive accumulation of the tracer was observed up to 110 and 220 min, respectively (Table 1). When radioactivity in these two organs was measured after they had been flushed with saline to remove the content, radioactivity substantially decreased, indicating that the progressive accumulation of the tracer resulted from gastrointestinal elimination in the faeces (Fig. 3).

From the peak concentration time, radioactivity progressively decreased in all tissues. In organs involved with tracer elimination (i.e. liver, small and large bowels, kidney and bladder), the decrease was, however, slower than in blood, leading to a progressive relative accumulation of the tracer. This phenomenon was also observed in the femur, oesophagus and stomach, although to a lesser extent.

Metabolism of the tracer

A relative quantitation of the native [^{18}F]EF3 and its metabolites was performed at various time points in the serum, the urine and the acetonitrile-soluble fraction of the muscle, liver, kidneys and NFSA tumours. The yield of processing (percentage of injected activity counted in the acetonitrile-soluble fraction) in these organs ranged from 85% in the muscle to 53% in the liver; it slightly decreased with time after tracer injection (data not shown).

Almost no metabolite was detected in the serum, muscle or urine early after injection, whereas in the liver and kidneys, the majority of the [^{18}F]EF3 was already metabolised (Table 2). With time, circulating metabolites were

Fig. 3. Tissue uptake in small (white boxes) and large bowel (black boxes) before (plain boxes) and after (hatched boxes) flushing with saline. Each bar represents the mean \pm 1 SD from four different mice. Statistically significant differences (Student's paired *t* test) are indicated with an asterisk

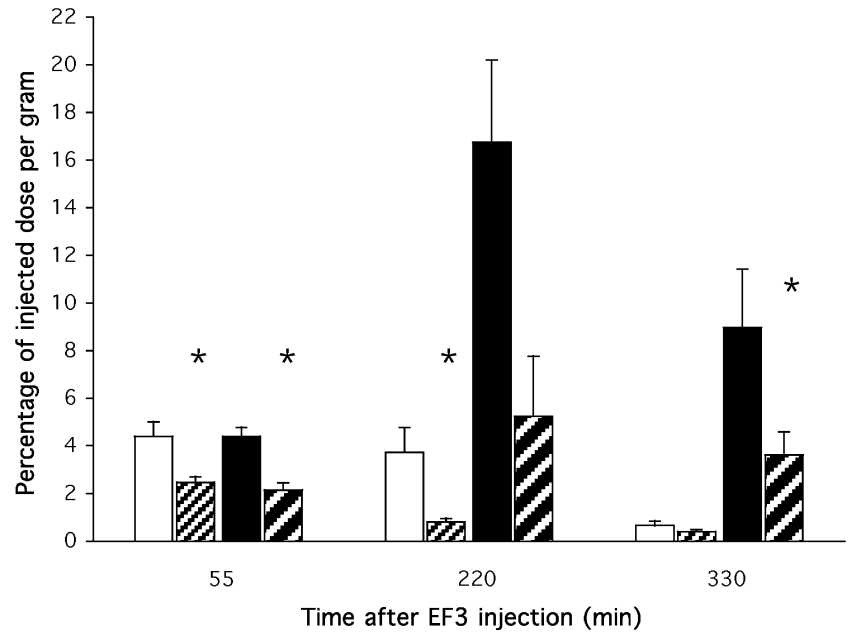


Table 1. Uptake of [^{18}F]EF3 (%ID/g of tissue) at various times after injection (mean \pm SEM of four different mice in normal tissues)

	5 min	55 min	110 min	220 min	330 min	440 min	550 min
Bladder	4.23 \pm 0.99	4.49 \pm 1.18	3.93 \pm 0.46	4.74 \pm 1.17	2.09 \pm 0.73	0.93 \pm 0.51	1.48 \pm 0.98
Blood	4.23 \pm 0.19	2.55 \pm 0.37	1.49 \pm 0.29	0.46 \pm 0.04	0.22 \pm 0.05	0.11 \pm 0.01	0.09 \pm 0.02
Brain	0.93 \pm 0.06	1.25 \pm 0.14	0.77 \pm 0.15	0.22 \pm 0.02	0.10 \pm 0.02	0.04 \pm 0.00	0.03 \pm 0.01
Oesophagus	2.85 \pm 0.59	1.53 \pm 0.74	1.74 \pm 0.14	0.51 \pm 0.07	0.31 \pm 0.12	0.28 \pm 0.00	0.18 \pm 0.02
Femoral bone	1.25 \pm 0.25	1.37 \pm 0.43	1.34 \pm 0.47	1.13 \pm 0.47	0.89 \pm 0.13	0.73 \pm 0.18	0.46 \pm 0.11
Heart	4.18 \pm 0.23	2.51 \pm 0.30	1.43 \pm 0.31	0.43 \pm 0.03	0.20 \pm 0.05	0.09 \pm 0.01	0.07 \pm 0.01
Kidney	7.02 \pm 0.61	5.92 \pm 1.02	6.16 \pm 0.54	3.76 \pm 0.71	1.99 \pm 0.37	1.91 \pm 0.45	1.33 \pm 0.14
Large bowel ^a	3.21 \pm 0.28	7.52 \pm 0.13	12.37 \pm 1.62	17.25 \pm 1.65	7.85 \pm 0.80	3.85 \pm 1.03	2.45 \pm 0.76
Liver	6.11 \pm 0.81	5.77 \pm 0.25	4.89 \pm 0.45	3.07 \pm 0.55	2.02 \pm 0.18	2.07 \pm 0.32	1.55 \pm 0.26
Lung	3.83 \pm 0.43	2.42 \pm 0.50	1.59 \pm 0.32	0.44 \pm 0.03	0.28 \pm 0.08	0.15 \pm 0.02	0.14 \pm 0.04
Muscle	3.62 \pm 0.24	2.18 \pm 0.41	1.21 \pm 0.16	0.35 \pm 0.04	0.17 \pm 0.03	0.12 \pm 0.04	0.06 \pm 0.02
Small bowel ^a	4.30 \pm 0.25	7.23 \pm 2.13	5.86 \pm 0.64	2.05 \pm 0.66	0.54 \pm 0.05	0.35 \pm 0.06	0.21 \pm 0.05
Spleen	3.58 \pm 0.33	2.28 \pm 0.28	1.32 \pm 0.30	0.37 \pm 0.04	0.19 \pm 0.05	0.09 \pm 0.01	0.07 \pm 0.02
Stomach ^a	3.13 \pm 0.16	2.68 \pm 0.40	1.52 \pm 0.29	0.54 \pm 0.09	0.19 \pm 0.03	0.17 \pm 0.02	0.13 \pm 0.03
FSA II tumours ^b	2.48 \pm 1.71	2.42 \pm 0.53	3.17 \pm 0.01	2.82 \pm 0.55	1.96 \pm 0.01	1.60 \pm 0.46	0.97 \pm 0.75
Sa-NH tumours ^b	2.99 \pm 0.90	2.67 \pm 0.32	1.60 \pm 0.04	1.33 \pm 0.83	0.62 \pm 0.55	0.60 \pm 0.29	0.83 \pm 0.53

^a GI tract not empty

^b Mean \pm SD of two tumours

Table 2. Percentage of native [^{18}F]EF3 at various times after injection (mean \pm SEM of four to nine different mice)

	30 min	55 min	220 min	330 min
NFSA tumour	49.3 \pm 9.1	58.2 \pm 18.2	54.2 \pm 10.5	55.0 \pm 0.3
Kidney	6.4 \pm 2.7	13.6 \pm 1.5	10.4 \pm 3.4	Not done
Liver	0.04 \pm 0.0	2.9 \pm 1.8	1.1 \pm 0.4	Not done
Muscle	85.4 \pm 3.5	76.4 \pm 2.0	67.9 \pm 10.9	Not done
Serum	92.3 \pm 2.3	78.3 \pm 5.4	70.9 \pm 3.2	Not done
Urine	77.7 \pm 1.3	72.5 \pm 1.9	52.3 \pm 2.4	Not done

measured in the serum and a progressive increase in the excretion of metabolites was observed in the urine. In NFSA tumours, half the radioactivity was associated with the native [^{18}F]EF3 without much change over time.

Uptake of [^{18}F]EF3 in SC tumours

In both Sa-NH and FSA II tumour models, the biodistribution of [^{18}F]EF3 was fast, with an uptake at 5 min which was not substantially different from that in the other normal tissues, the brain, femur, kidneys and liver

Fig. 4. TBRs in FSA II (black bars) and Sa-NH (white bars) tumours at various times after [¹⁸F]EF3 injection. Bars represent the mean from two different mice

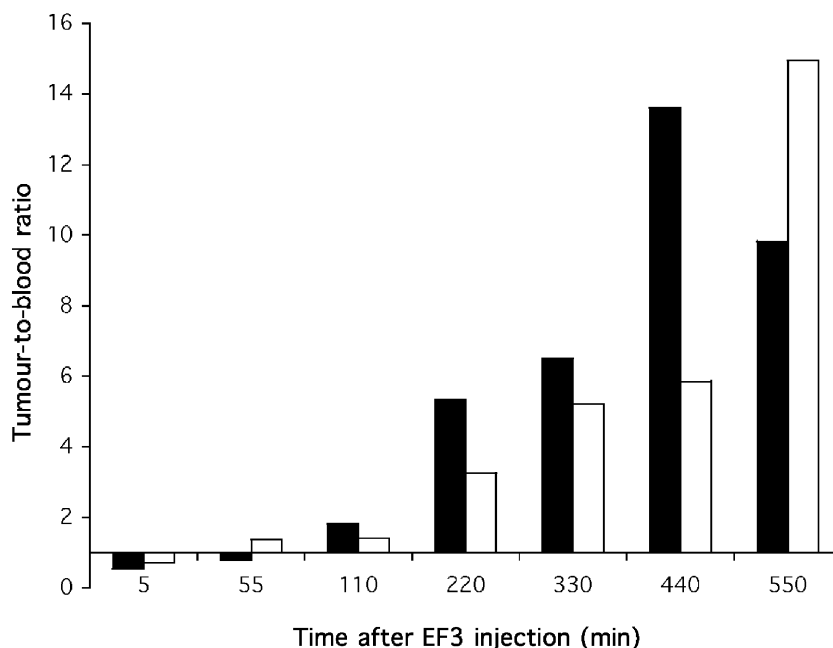


Table 3. [¹⁸F]EF3 uptake at 220 min after injection (mean±SEM of 4–18 different mice)

	FSA	NFSA	FSA II	SCC VII	Sa-NH	MCA-4
Percentage of injected dose/g						
In blood	2.03±0.34	0.57±0.07	0.73±0.26	0.68±0.07	1.02±0.33	0.34±0.04
In muscle	1.92±0.26	0.52±0.05	0.61±0.19	0.60±0.07	0.45±0.08	0.29±0.04
In tumours	2.39±0.34	0.78±0.08	1.11±0.23	1.48±0.16	1.06±0.11	1.00±0.13
Tumour-to-muscle ratio	1.31±0.04	1.62±0.15	2.47±0.27	2.55±0.07	2.62±0.24	3.52±0.29
Tumour-to-blood ratio	1.24±0.05	1.38±0.15	2.08±0.18	2.19±0.14	1.97±0.45	2.88±0.18

excepted (Table 1). There was a progressive relative accumulation of the tracer in both tumours, as illustrated by the increase in TBR with time (Fig. 4). Two hundred and twenty minutes after the injection, the radioactivity was higher in SC FSA II and Sa-NH tumours than in the organs not involved in tracer excretion (blood, oesophagus, heart, lung, muscle, spleen and stomach) (ANOVA, $p < 0.001$, compared with $p = 0.06$, 0.70 and 0.22, at 5, 55 and 110 min and to $p < 0.001$ at 330, 440 and 550 min after tracer injection). TBR remained higher in FSA II tumours than in Sa-NH tumours for almost all times investigated.

Ranking of hypoxia among various IM tumour types

Under ambient air (21% O₂), 220 min after injection, [¹⁸F]EF3 activity was significantly higher in all tumour models than in the muscle of the contralateral limb or the blood, resulting in TMR or TBR values above unity (Table 3). For both TMR and TBR, the inter-strain coefficients of variation (CV) were larger than the intra-strain CV. For TMR, intra-strain CV reached 5.7%,

17.9%, 42.9%, 33.0%, 18.7% and 18.5%, for FSA, NFSA, FSA II, SCC VII, Sa-NH and MCA-4, respectively, whereas inter-strain reached 57.5%. For TBR, corresponding values reached 7.3%, 21.3%, 30.4%, 25.9%, 45.6% and 14.0% for intra-strain CV, and 55.6% for inter-strain CV, respectively.

Uptake of [¹⁸F]EF3 under different oxygenation conditions

At 55 min after tracer injection, no change in TMR was observed under 10% O₂ or carbogen, either in FSA II or in SCC VII tumours (Fig. 5). At later times after injection, in FSA II tumours, under 10% O₂ breathing, TMR increased, whereas it decreased under carbogen breathing. It only reached a level of significance at 220 min after tracer injection.

In SCC VII tumours, at 220 min after tracer injection, there was a trend towards an increase in the TMR under 10% O₂ breathing ($p = 0.08$), and a decrease in TMR under carbogen breathing ($p = 0.06$). At later time points, data were scattered and a difference in TMR was no longer observed.

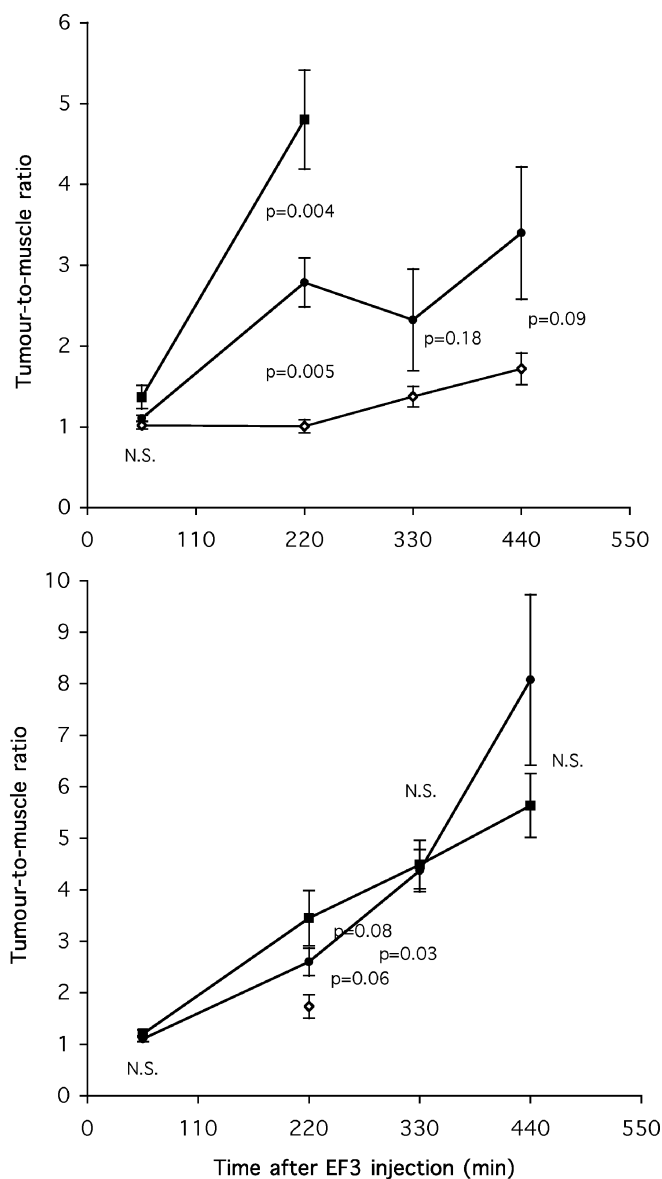


Fig. 5. TMRs of [¹⁸F]EF3 uptake under 10% O₂ (filled squares), 21% O₂ (filled circles) or carbogen (open circles) in FSA II (upper panel) or SCC VII (lower panel) tumour-bearing mice. Each data point represents the mean±SEM of 4–21 mice. Statistical differences were evaluated by Student's *t* test

Discussion

This article reports on the pharmacokinetics, biodistribution and specificity for hypoxia of the positron-labelled tri-fluorinated nitroimidazole derivative [¹⁸F]EF3 in murine normal tissues and tumours. This tracer has a mono-exponential blood clearance without accumulation in the red blood cells (Fig. 1). It is rapidly metabolised in the liver and kidney (Table 2), and it is eliminated mainly via the urinary tract as a mixture between the native compounds and metabolites, and to a lesser extent via the gastrointestinal tract (Fig. 2). [¹⁸F]EF3 has a fast and

even biodistribution in normal tissues, except in the brain and the bone (Table 1). With time, it is progressively cleared from all normal tissues (Table 1) except the kidneys, bladder and gastrointestinal tract, where it accumulates into the faeces (Fig. 3). [¹⁸F]EF3 also has a fast biodistribution in SC tumours followed by a progressive relative accumulation with time after tracer injection (Table 1, Fig. 4). Finally, at 220 min after injection, [¹⁸F]EF3 was able to discriminate tumours with different hypoxic fractions (Table 3), as well as environmental conditions modifying tumour hypoxia (Fig. 5).

Homogeneous and fast biodistribution of [¹⁸F]EF3 in mice has been observed even in the brain, although to a lesser extent. This finding is not surprising given the relative lipophilicity of the drug. The octanol-to-buffer partition coefficient of EF3 has been measured at 1.12 (A. Cheguillaume, personal communication), which compares with 0.17 for FETNIM, 0.4 for F-MISO, 0.35 for EF1 and 5.7 for EF5 [24, 28]. Typically, more hydrophilic drugs have a more heterogeneous biodistribution, especially in the central nervous system, and are more rapidly eliminated, preferentially via the urinary tract [29, 33]. Comparison of the various hypoxia tracers with regard to their biodistribution and elimination is a difficult task as they have been studied in different animal models using different experimental protocols. However, using a mono-exponential elimination model applied to published data in rats, half-lives of 98, 108 and 150 min have been recalculated for [¹⁸F]MISO, [¹⁸F]FETNIM and [¹⁸F]EF5, respectively [24, 33, 34]. Also, in comparison with [¹⁸F]FETNIM, [¹⁸F]EF3 exhibited a higher liver uptake [33]. Finally, a lower brain uptake of [¹⁸F]FETNIM and [¹⁸F]EF1 has been observed compared with [¹⁸F]EF3 or [¹⁸F]EF5 [28, 29, 33]. Experiments are in progress in our laboratory in collaboration with another research group to compare [¹⁸F]EF3, [¹⁸F]MISO, [¹⁸F]EF5 and possibly [¹⁸F]FETNIM in similar animal models and experimental conditions.

A homogeneous biodistribution without doubt represents an interesting characteristic for a hypoxia tracer, as it increases the probability of an even diffusion, especially in tumours, where the vascularisation is typically abnormal [27]. In the two murine sarcomas investigated over an entire time course, [¹⁸F]EF3 uptake was fast and not substantially different from that in the other tissues, with the exception of the kidneys, bladder and gastrointestinal tract, in which it was higher, and the femur and brain, in which it was slightly lower (Table 1). With time, progressive elimination of the tracer was observed in all tissues. In the small and large bowel, this elimination was only apparent after the organs had been flushed to remove the faeces in which the tracer accumulated (Fig. 3). The rate of tracer elimination was, however, different from tissue to tissue, leading to a progressive accumulation in tumours but also in normal tissues such as the oesophagus and femoral bone. We have no clear explanation for these latter findings. Accumulation of

pimonidazole and EF5 in the oesophagus has also been reported [35, 36]. Whether this accumulation reflects some degree of hypoxia in the oesophagus, as suggested by LD₅₀ experiments [37], or unspecific binding is unknown at present. However, Cobb et al. described very high nitroreductase activities inducing retention of miso-nidazole in tissues like oesophagus [38, 39]. Regarding bone accumulation, we have ruled out defluorination into free ¹⁸F, which is known to specifically accumulate into bones [40].

Interestingly, [¹⁸F]EF3 accumulated in all six murine tumours investigated relative to the blood and muscle activity. All these tumours are known to present various degrees of hypoxia as measured by polarographic probes or immunofluorescence on tissue sections after EF5 administration (C. Milross, personal communication) [41, 42]. These measurements were performed under different experimental conditions (e.g. different tumour size, use of general anaesthesia, SC or IM tumours) and are not available for all tumour types; hence a direct comparison between the various methods is probably inappropriate. However, in the case of FSA and MCA-4 tumours, which rank at the extremes of the TMR (or TBR) values, median pO₂ values of 12.8 and 5.0 mmHg have been reported for IM tumours [41]. Using the fluorescence intensity of EF5 adducts, which has been shown to vary with the absolute tissue pO₂ values, in the murine tumours used in the present experiments a correlation was observed ($r^2=0.57$, $p<0.05$) on an average basis between the mean fluorescence intensity and the [¹⁸F]EF3 relative uptake expressed by the TMR (data not shown) [32, 42]. A comparison on an individual tumour basis between [¹⁸F]EF3 uptake and immunofluorescence of EF5 adducts is in progress in our laboratory.

The specificity of [¹⁸F]EF3 for hypoxia is further illustrated by the experiments in which the environmental conditions were modified to vary the hypoxic fraction. In FSA II tumours, the tracer uptake depended to a large extent on the oxygenation conditions, i.e. it increased under 10% O₂ breathing and decreased close to unity under carbogen breathing. In SCC VII tumours, such an effect was, however, only observed at 220 min after tracer injection. The reason for the absence of a difference for later time points is not known. Variation in tumour perfusion is probably not involved as no difference in TMR was observed between the various experimental conditions at 55 min after tracer injection, whereas the micro-environment (and thus potentially the perfusion) had already been changed for almost an hour. Re-uptake of tracer metabolites in normal tissues is an explanation that is being looked at by characterising these metabolites with mass spectroscopy analyses.

Further indirect evidence for the oxygen dependency of the uptake and retention of [¹⁸F]EF3 is provided by the finding that FSA II and Sa-NH tumours exhibited higher TMR when implanted subcutaneously than when implanted intramuscularly. It is typically considered that

IM tumours are better vascularised, and therefore are less hypoxic, than SC tumours [41]. These data also indirectly rule out the hypothesis that differences in tumour perfusion explain to a large extent the variation in [¹⁸F]EF3 uptake and retention among different tumour types and/or under different oxygenation conditions.

Preclinical experiments by Chapman on iodo-azomycin-galactoside (IAZG) suggested that the highest sensitivity for the detection of hypoxia occurred after renal excretion of unbound tracer [43], leading to minimal background in tissues. Knowing that the optimal time for imaging hypoxia is dictated by the half-life of the isotope, it is reasonable to say that in vivo image acquisition should ideally start within two half-lives, namely within 220 min for fluorine-labelled PET tracers. In this regard, tracers labelled with longer half-life isotopes, such as [¹²⁴I]IAZG, might have an intrinsic advantage [44]. Comparison of this tracer with [¹⁸F]F-MISO in animal models has recently shown its potential for hypoxia imaging. However, dehalogenation, worse image resolution with [¹²⁴I] and higher administered activities remain a matter of concern.

It is important to take into account the metabolism of a tracer when interpreting preclinical or clinical data, as detection with PET or SPECT does not allow distinction between the native compound and its metabolites. The presence of metabolites will increase the background signal and thus limit the sensitivity of the tracer for the detection of tissue hypoxia. According to our data, [¹⁸F]EF3 is mainly metabolised in the liver and kidneys and eliminated partly as native compound and partly as metabolites. Interestingly, few circulating metabolites were measured in the blood and muscles, and the overall background activity was accordingly limited. Whereas with [¹⁸F]FETNIM the proportion of unchanged molecule in plasma remained constant over time, the percentage as well as the absolute concentration of native [¹⁸F]EF3 in serum decreased with time (Fig. 1, Table 2) [33]. In tumours, about half the radioactivity came from metabolites. Large variations in the proportion of metabolites were, however, observed, confirming the heterogeneity of tumours compared with normal tissues. The same phenomenon has been reported for [¹⁸F]FETNIM, with wide variation, from 3% to 70%, in the radioactivity represented by unchanged molecule in DMDA-induced tumours [33]. Characterisation of the EF3 metabolites by mass spectroscopy analyses is in progress. It may well be that these metabolites are reduced unbound [¹⁸F]EF3 which is progressively cleared from the tumours. If so, the radioactive signal in tumours (resulting from the bound and unbound tracer) will still be proportional to the oxygen concentration.

All these findings contrast with data on F-MISO, which circulates to a significant extent in the blood as metabolites [45]. In human patients, only 3% of the injected dose of F-MISO was excreted unchanged in urine [46] compared with 70% of parent EF5 [47]. In our C3H

mouse models, $\pm 40\%$ of the injected dose of [^{18}F]EF3 was excreted unchanged, and $\pm 30\%$ was excreted as metabolites (extrapolation from HPLC data in urine at 30, 55 and 220 min to volumes of urine collected over the entire time course between 5 and 770 min).

In summary, with its fast and even biodistribution in normal tissues and tumours, its low fraction of circulating metabolites and its progressive and oxygen-dependent accumulation in tumours relative to that in blood and muscle, [^{18}F]EF3 appears a good candidate for detection of tissue hypoxia with PET. Further experiments aiming to confirm the relationship between relative tracer accumulation and hypoxic fraction are ongoing in various murine tumour models. [^{18}F]EF3 has recently been introduced into our clinic, where a phase I trial for patients with head and neck squamous cell carcinoma is in progress.

Acknowledgements. This work was initiated thanks to a collaboration with Prof. C. Koch, Radiation Oncology Dept., School of Medicine, University of Pennsylvania, Philadelphia, USA. It was supported by research grants from the "Fonds de la Recherche Scientifique Médicale" of Belgium (grants #3.4571.95, 3.4610.99 and 3.4560.00), by a research contract with the Region of Wallonia and by grants from the "Fonds Joseph Maisin", Brussels, Belgium. The authors wish to thank Prof. B. Gallez and Dr. Sc. J. Gueulette for fruitful discussions during acquisition and analysis of the data, and Profs. F. Jamar and S. Pauwels for the use of their nuclear medicine facility.

References

- Horsman MR, Nordsmark M, Overgaard J. Techniques to assess the oxygenation of human tumors. State of the art. *Strahlenther Onkol* 1998;174(Suppl 4):2–5
- Kennedy AS, Raleigh JA, Perez GM, et al. Proliferation and hypoxia in human squamous cell carcinoma of the cervix: first report of combined immunohistochemical assays. *Int J Radiat Oncol Biol Phys* 1997;37:897–905
- Hodgkiss RJ. Use of 2-nitroimidazoles as bioreductive markers for tumour hypoxia. *Anticancer Drug Des* 1998;13:687–702
- Busch TM, Hahn SM, Evans SM, Koch CJ. Depletion of tumor oxygenation during photodynamic therapy: detection by the hypoxia marker EF3 [2-(2-nitroimidazole-1[H]-yl)-N-(3,3,3-trifluoropropyl)acetamide]. *Cancer Res* 2000;60:2636–2642
- Koch CJ. Measurement of absolute oxygen levels in cells and tissues using oxygen sensors and 2-nitroimidazole EF5. *Methods Enzymol* 2002;352:3–31
- Raleigh JA, Koch CJ. The importance of thiols in the reductive binding of 2-nitroimidazoles to macromolecules. *Biochem Pharmacol* 1990;40:2457–2464
- Kaanders JHAM, Wijffels KIEM, Marres HAM, Pop LAM, Marres HAM, Ljungkvist ASE, Pop LAM, van den Hoogen FJA, de Wilde PCM, Bussink J, Raleigh JA, van der Kogel AJ. Pimonidazole binding and tumor vascularity predict for treatment outcome in head and neck cancer. *Cancer Res* 2002;62:7066–7074
- Evans SM, Judy KD, Dunphy I, Nelson P, Magarelli D, Jenkins WT, Hahn SM, Collins RM, Koch CJ. Hypoxia, as measured by EF5 binding, predicts recurrence in adult brain tumors. *Int J Radiat Oncol Biol Phys* 2003;55:470
- Tubis M, Krishnamurthy G, Endow JS, Stein RA, Suwanik R, Bland WH. Labeled metronidazole as potential agents for amebic abscess imaging. *J Nucl Med* 1975;14:163–171
- Chapman JD, Franko AJ, Koch CJ. The fraction of hypoxic clonogenic cells in tumor populations. In: Nervi C, Arcangeli G, Mauro F, eds. *Proceedings of the Second Rome International Symposium (1980): biological bases and clinical implications of tumor radioresistance*. New York: Masson; 1983:61–73
- Ballinger JR. Imaging hypoxia in tumors. *Semin Nucl Med* 2001;31:321–329
- Rasey JS, Grunbaum Z, Magee S, et al. Characterization of radiolabeled fluoromisonidazole as a probe for hypoxic cells. *Radiat Res* 1987;111:292–304
- Rasey JS, Koh WJ, Grierson JR, Grunbaum Z, Krohn KA. Radiolabeled fluoromisonidazole as an imaging agent for tumor hypoxia. *Int J Radiat Oncol Biol Phys* 1989;17:985–991
- Rasey JS, Casciari JJ, Hofstrand PD, Muzi M, Graham MM, Chin LK. Determining hypoxic fraction in a rat glioma by uptake of radiolabeled fluoromisonidazole. *Radiat Res* 2000;153:84–92
- Koh WJ, Rasey JS, Evans ML, Grierson JR, Lewellen TK, Graham MM, Krohn KA, Griffin TW. Imaging of hypoxia in human tumors with [^{18}F]fluoromisonidazole. *Int J Radiat Oncol Biol Phys* 1992;22:199–212
- Valk PE, Mathis CA, Prados MD, Gilbert JC, Budinger TF. Hypoxia in human gliomas: demonstration by PET with fluorine-18-fluoromisonidazole. *J Nucl Med* 1992;33:2133–2137
- Koh WJ, Bergman KS, Rasey JS, et al. Evaluation of oxygenation status during fractionated radiotherapy in human nonsmall cell lung cancers using [^{18}F]fluoromisonidazole positron emission tomography. *Int J Radiat Oncol Biol Phys* 1995;33:391–398
- Rasey JS, Koh WJ, Evans ML, Peterson LM, Lewellen TK, Graham MM, Krohn KA. Quantifying regional hypoxia in human tumors with positron emission tomography of [^{18}F]fluoromisonidazole: a pretherapy study of 37 patients. *Int J Radiat Oncol Biol Phys* 1996;36:417–428
- Yeh SH, Liu RS, Wu LC, Yang DJ, Yen SH, Chang CW, Yu TW, Chou KL, Chen KY. Fluorine-18 fluoromisonidazole tumour to muscle retention ratio for the detection of hypoxia in nasopharyngeal carcinoma. *Eur J Nucl Med* 1996;23:1378–1383
- Shelton ME, Dence CS, Hwang DR, Herrero P, Welch MJ, Bergmann SR. In vivo delineation of myocardial hypoxia during coronary occlusion using fluorine-18 fluoromisonidazole and positron emission tomography: a potential approach for identification of jeopardized myocardium. *J Am Coll Cardiol* 1990;16:477–485
- Read SJ, Hirano T, Abbott DF, Sachinidis JI, Tochon-Danguy HJ, Chan JG, Egan GF, Scott AM, Bladin CF, McKay WJ, Donnan GA. Identifying hypoxic tissue after acute ischemic stroke using PET and ^{18}F -fluoromisonidazole. *Neurology* 1998;51:1617–1621
- Liu RS, Chu LS, Yen SH, Chang CP, Chou KL, Wu LC, Chang CW, Lui MT, Chen KY, Yeh SH. Detection of anaerobic odontogenic infections by fluorine-18 fluoromisonidazole. *Eur J Nucl Med* 1996;23:1384–1387

23. Tewson TJ. Synthesis of [¹⁸F]fluoroetanidazole: a potential new tracer for imaging hypoxia. *Nucl Med Biol* 1997;24:755–760
24. Yang DJ, Wallace S, Cherif A, Li C, Gretzer MB, Kim EE, Podoloff DA. Development of F-18-labeled fluoroerythronitroimidazole as a PET agent for imaging tumor hypoxia. *Radiology* 1995;194:795–800
25. Lehtio K, Oikonen V, Gronroos T, Eskola O, Kalliokoski K, Bergman J, Solin O, Grenman R, Nuutila P, Minn H. Imaging of blood flow and hypoxia in head and neck cancer: initial evaluation with [¹⁵O]H₂O and [¹⁸F]fluoroerythronitroimidazole PET. *J Nucl Med* 2001;42:1643–1652
26. Lehtio K, Oikonen V, Nyman S, Grönroos T, Roivainen A, Eskola O, Minn H. Quantifying tumour hypoxia with fluorine-18 fluoroerythronitroimidazole ([¹⁸F]FETNIM) and PET using the tumour to plasma ratio. *Eur J Nucl Med Mol Imaging* 2003;30:101–108
27. Dewhirst MW. Concepts of oxygen transport at the microcirculatory level. *Semin Radiat Oncol* 1998;8:143–150
28. Ziemer LS, Evans SM, Kachur AV, Shuman AL, Cardi CA, Jenkins WT, Karp JS, Alavi A, Dolbier WR Jr, Koch CJ. Non-invasive imaging of tumor hypoxia in rats using the 2-nitroimidazole ¹⁸F-EF5. *Eur J Nucl Med Mol Imaging* 2003;30:259–266
29. Evans SM, Kachur AV, Shiue CA, Hustinx R, Jenkins WT, Shive GG, Karp JS, Alavi A, Lord EM, Dolbier WR Jr, Koch CJ. Noninvasive detection of tumor hypoxia using the 2-nitroimidazole [¹⁸F]EF1. *J Nucl Med* 2000;41:327–336
30. Josse O, Labar D, Georges B, Grégoire V, Marchand J. Synthesis of [¹⁸F]-labelled EF3 [2-(2-nitroimidazol-1-yl)-N-(3,3,3-trifluoropropyl)-acetamide], a marker for PET detection of hypoxia. *Bioorg Med Chem* 2001;9:665–675
31. Milas L, Hunter N, Mason K, Withers HR. Immunological resistance to pulmonary metastases in C3Hf/Bu mice bearing syngeneic fibrosarcoma of different sizes. *Cancer Res* 1974;34:61–71
32. Mahy P, De Bast M, Gallez B, Gueulette J, Koch CJ, Scalliet P, Grégoire V. In vivo colocalisation of 2-nitroimidazole EF5 fluorescence intensity and electron paramagnetic resonance oximetry in mouse tumors. *Radiother Oncol* 2003;67:53–61
33. Gronroos T, Eskola O, Lehtio K, Minn H, Marjamaki P, Bergman J, Haaparanta M, Forsback S, Solin O. Pharmacokinetics of [¹⁸F]FETNIM: a potential marker for PET. *J Nucl Med* 2001;42:1397–1404
34. Evans SM, Jenkins WT, Joiner B, Lord EM, Koch CJ. 2-Nitroimidazole (EF5) binding predicts radiation resistance in individual 9L s.c. tumors. *Cancer Res* 1996;56:405–411
35. Cobb LM, Nolan J, Butler SA. Distribution of pimonidazole and RSU 1069 in tumour and normal tissues. *Br J Cancer* 1990;62:915–918
36. Laughlin KM, Evans SM, Jenkins WT, et al. Biodistribution of the nitroimidazole EF5 (2-[2-nitro-1*H*-imidazol-1-yl]-*N*-(2,2,3,3,3-pentafluoropropyl) acetamide) in mice bearing subcutaneous EMT6 tumors. *J Pharmacol Exp Ther* 1996;277:1049–1057
37. Phillips TL, Ross G. Time-dose relationships in the mouse esophagus. *Radiology* 1974;113:435–440
38. Cobb LM, Nolan J, Butler S. Tissue distribution of ¹⁴C- and ³H-labelled misonidazole in the tumor-bearing mouse. *Int J Radiat Oncol Biol Phys* 1990;18:347–351
39. Cobb LM, Nolan J, Hacker T. Retention of misonidazole in normal and malignant tissues: interplay of hypoxia and reductases. *Int J Radiat Oncol Biol Phys* 1992;22:655–659
40. Petren-Mallmin M, Andreasson I, Ljunggren O, Ahlstrom H, Bergh J, Antoni G, Langstrom B, Bergstrom M. Skeletal metastases from breast cancer: uptake of ¹⁸F-fluoride measured with positron emission tomography in correlation with CT. *Skeletal Radiol* 1998;27:72–76
41. Milross CG, Peters LJ, Hunter NR, Mason KA, Tucker SL, Milas L. Polarographic pO₂ measurement in mice: effect of tumor site, site of implantation, and anesthesia. *Rad Oncol Invest* 1996;7:108–114
42. Mahy P, Gueulette J, Scalliet P, Grégoire V. Quantitative detection of EF5 adducts with immunofluorescence (IF) and flow cytometry (FC) to measure hypoxia in murine tumors. *Cancer Res* 1999;40:641
43. Chapman JD, Engelhardt EL, Stobbe CC, Schneider RF, Hanks GE. Measuring hypoxia and predicting tumor radioresistance with nuclear medicine assays. *Radiother Oncol* 1998;46:229–237
44. Zanzonico P, O'Donoghue J, Chapman JD, Schneider R, Cai S, Larson S, Wen B, Chen Y, Finn R, Ruan S, Gerweck L, Humm J, Ling C. Iodine-124-labeled iodo-azomycin-galactoside imaging of tumor hypoxia in mice with serial microPET scanning. *Eur J Nucl Med Mol Imaging* 2004;31:117–128
45. Rasey JS, Hofstrand PD, Chin LK, Tewson TJ. Characterization of [¹⁸F]fluoroetanidazole, a new radiopharmaceutical for detecting tumor hypoxia. *J Nucl Med* 1999;40:1072–1079
46. Graham MM, Peterson LM, Link JM, Evans ML, Rasey JS, Koh WJ, Caldwell JH, Krohn KA. Fluorine-18-fluoro-misonidazole radiation dosimetry in imaging studies. *J Nucl Med* 1997;38:1631–1636
47. Koch CJ, Hahn SM, Rockwell Jr K, Covey JM, McKenna WG, Evans SM. Pharmacokinetics of EF5 [2-(2-nitro-1-*H*-imidazol-1-yl)-*N*-(2,2,3,3,3-pentafluoropropyl) acetamide] in human patients: implications for hypoxia measurements in vivo by 2-nitroimidazoles. *Cancer Chemother Pharmacol* 2001;48:177–187